1-1-2014

Molecular dynamics study on the atomic mechanisms of coupling motion of [0 0 1] symmetric tilt grain boundaries in copper bicrystal

Liang Zhang
University of Wollongong, lz592@uowmail.edu.au

Cheng Lu
University of Wollongong, chenglu@uow.edu.au

Guillaume Michal
University of Wollongong, gmichal@uow.edu.au

A Kiet Tieu
University of Wollongong, ktieu@uow.edu.au

Kuiyu Cheng
University of Wollongong, kc938@uowmail.edu.au

Molecular dynamics study on the atomic mechanisms of coupling motion of [0 0 1] symmetric tilt grain boundaries in copper bicrystal

Abstract

Recent research has revealed that some grain boundaries (GBs) can migrate coupled to applied shear stress. In this paper, molecular dynamics (MD) simulations were performed on sixteen [0 0 1] symmetric tilt GBs of bicrystal Cu to identify atomic-scale GB migration mechanisms and investigate their dependence on GB structure. The misorientation angles (θ) of the sixteen GBs cover the interval from 0° to 90° and a wide range of Σ values. A general method was proposed to explore the possible GB structures for each misorientation angle. Molecular statics simulation at a temperature of 0K were carried out first to determine the equilibrium and some possible metastable structures of the sixteen investigated [0 0 1] GBs. MD simulations were then conducted on the bicrystal models at equilibrium by applying a shear strain parallel to the GB plane. Shear deformation caused the tangential translation of the grain and induced normal motion of the GBs. This boundary coupling motion was present in the entire range of misorientation angles. Different mechanisms of coupled boundary motion at atomic scale were carefully examined in this work. The common feature of these mechanisms can be regarded as the displacement of local atoms and rotation of certain structure unit. Structure phase transformation of GB was found during the migration of Σ17(4 1 0) and Σ73 (8 3 0) GBs.

Keywords

copper, boundaries, grain, tilt, symmetric, 1, motion, coupling, bicrystal, mechanisms, molecular, atomic, study, dynamics

Disciplines

Arts and Humanities | Law

Publication Details

Zhang, L., Lu, C., Michal, G., Tieu, A. Kiet. and Cheng, K. (2014). Molecular dynamics study on the atomic mechanisms of coupling motion of [0 0 1] symmetric tilt grain boundaries in copper bicrystal. Materials Research Express, 1 (1), 015019.

Molecular Dynamics Study on the Atomic Mechanisms of Coupling Motion of [0 0 1] Symmetric Tilt Grain Boundaries in Copper Bicrystal

Liang Zhang, Cheng Lu, Guillaume Michal, Kiet Tieu, Kuiyu Cheng

School of Mechanical, Materials and Mechatronic Engineering, University of Wollongong, Wollongong, NSW 2522, Australia

Abstract:

Recent research has revealed that some grain boundaries (GBs) can migrate coupled to applied shear stress. In this paper, molecular dynamics (MD) simulations were performed on sixteen [0 0 1] symmetric tilt GBs of bicrystal Cu to identify atomic-scale GB migration mechanisms and investigate their dependence on GB structure. The misorientation angles (θ) of the sixteen GBs cover the interval from 0° to 90° and a wide range of ∑ values. A general method was proposed to explore the possible GB structures for each misorientation angle. Molecular statics simulation at a temperature of 0K were carried out first to determine the equilibrium and some possible metastable structures of the sixteen investigated [0 0 1] GBs. MD simulations were then conducted on the bicrystal models at equilibrium by applying a shear strain parallel to the GB plane. Shear deformation caused the tangential translation of the grain and induced normal motion of the GBs. This boundary coupling motion was present in the entire range of misorientation angles. Different mechanisms of coupled boundary motion at atomic scale were carefully examined in this work. The common feature of these mechanisms can be regarded as the displacement of local atoms and rotation of certain structure unit. Structure phase transformation of GB was found during the migration of ∑17(4 1 0) and ∑73 (8 3 0) GBs.

Keywords: Molecular Dynamics; Nanocrystalline; Grain boundary; Atomic mechanism; Copper

1. Introduction

Grain boundaries (GBs) constitute the interfaces between different oriented crystals of the same material. They are important microstructural features of polycrystalline materials that impact the bulk properties [1], especially when the grain size is reduced to nano scale. Many research works [2-5] indicated that the dislocation activities in the interior of grains lessen when the average grain size is less than 100 nm whereas mechanisms mediated by the GB become dominant. The reported alternative deformation mechanisms of nanocrystalline metals includes: GB sliding [6], grain rotation [7, 8], diffusional creep [9], GB migration [10-12], dislocation nucleation or absorption at GB [13-17]. To gain a deeper understanding of the role of GBs, their structures must be precisely characterized.

The atomic structure and energy of GBs have been studied for many years. The boundary energy in Cu has been experimentally determined by transmission electron microscopy (TEM) as a function of the misorientation angle for [1 0 0] and [1 1 0] twist boundaries [18], and symmetric tilt boundaries of [1 0 0] and [1 1 0] [19]. The results showed strong correlations between the GB atomic structure and GB energy. Experiments demonstrated that some specific low energy structures of GBs are the preferred configurations in polycrystalline materials [20, 21]. However, experimental observation by TEM is extremely difficult [22-24], especially at high temperatures, since diffusion phenomena and interfacial transitions deeply modify the low-temperature structure and properties of GBs. Atomic simulation has been widely used to provide insight in the relationship between GB energy and their atomic structures in recent times. Wolf investigated the [1 0 0], [1 1 1], [1 1 0], [1 1 3] and [1 1 2] tilt and twist GBs as well as asymmetric twist GBs [25-28]. Rittner and Seidman researched on twenty-one symmetric tilt grain boundaries along [1 1 0] axis with atomistic simulations [29]. Sangid et al. conducted a series of molecular dynamic (MD) simulation works on Ni for various symmetric twist and tilt GB angles around different axis [30].

Grain boundary motion coupled to shear deformation was widely observed for both low misorientation angle GBs [31, 32] and high misorientation angle GBs [11, 12, 33-39] in a number of metallic materials. The coupled GB migration plays an important role in grain growth [40, 41], nucleation of new grains during recrystallization [42] and thermo-mechanical processing of materials [1]. Mishin and coworkers investigated the GB coupling motion using the atomic simulation method [10, 43, 44]. They found that the coupling effect can be characterized by a geometric constant factor β

representative of the GB structure [10]. Simulations corroborate very well the coupling factors obtained experimentally from bicrystals [45, 46]. However, very little is known about the atomic-scale mechanisms involved.

The purpose of the present paper is to identify the mechanism of GB migration at atomic-scale and investigate its dependence on GB structure by computational simulations. Sixteen different symmetric GBs of Cu tilted around the [0 0 1] axis are investigated. The misorientation angles spanned from 0° to 90°. Firstly, the method of construction of the sample and the simulation are introduced in section 2. In section 3, the detailed GB configurations are studied and their energy are calculated. The results of coupling GB motion to shear deformation are presented and the GB coupling mechanisms at atomic-scale are discussed.

2. Simulation method

The GB structure is a function of five macroscopic geometrical degrees of freedom (DOF) defined as the rotation axis **c**, the rotation angle θ and the boundary plane unit normal **n**. Because bicrystal systems enable a more controlled investigation of specific GB properties, previous simulations harnessed this advantage to study the mechanical properties of GB [47-50]. This approach was followed in the present study. All Cu bicrystals used in the following have a symmetric tilt misorientation about [0 0 1] axis. A typical bicrystal interface simulation model is shown in Figure 1.

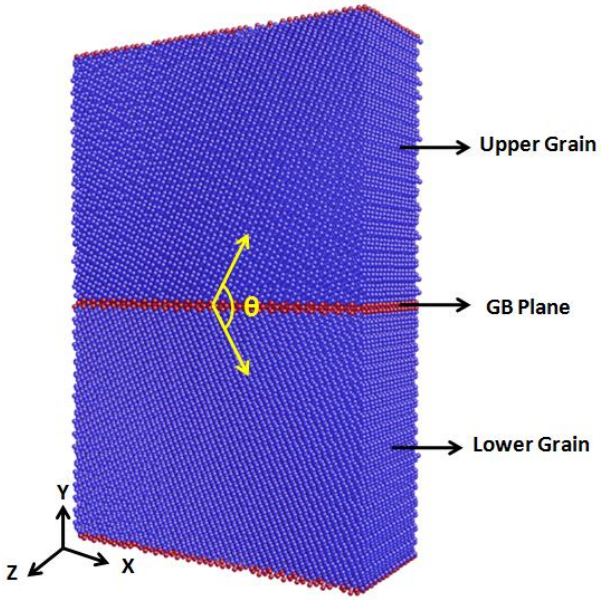

Figure 1 A typical bicrystal interface model. The interface is created by a symmetric tilt rotation of the upper and lower grain around the [0 0 1] axis. The atoms with blue color form a perfect fcc lattices. The atoms colored red in the middle of the model define the grain boundary plane.

In the bicrystal simulation models, the [0 0 1] crystallographic direction was parallel to the Z-axis, which is defined as the tilt axis. The [1 0 0] crystallographic direction was originally aligned with the X-axis. A symmetric tilt grain boundary was formed around the middle plane along the Y-axis by rotating lattices in the upper half part of the model around the tilt axis by θ/2 counterclockwise and those in the lower half part of the model by θ/2 clockwise. Two grains were generated in the upper half part and lower half part of the model, respectively. Sixteen cases with different rotation angles (θ), as shown in Table 1, have been simulated. It is known that a certain number of the atoms having coincidental locations in both grains form coincident site lattices (CSL) [1]. Each symmetric tilt GB can be characterized by the reciprocal of the fraction of coincidental sites ∑. Table 1 presents the values for ∑ for the sixteen simulation cases. The value in the parentheses indicates the crystallographic direction of the upper grain parallel to the X-axis. The simulation models had two dimensional periodic boundary conditions along the X and Z directions. The non-periodic boundary condition was applied to the Y direction.

The possible influence of the bicrystal model scale on the simulation result are fully considered in this work. Specifically, the width of the interface in X direction should be long enough to produce a serials of interface periods from which the boundary structures can be generally predicted. The length of the bicrystal model in Y direction should be considered to avoid the interaction of the two boundary planes which can affect the nucleation stress and the character of the nucleated partial dislocation [51]. Furthermore, if the thickness of the bicrystal model in Z direction is reduced to a few

atomic planes, dislocation will be restricted to occur on certain slip system [52]. In this study, the length of each simulation model was about 144 Å in the X direction and 54 Å in the Z direction. The model length along the Y direction was set to about 216 Å. The total number of atoms in each simulation model was close to 140,000.

Table 1 Boundary energies for different [0 0 1] symmetric tilt grain boundaries of Cu bicrystal at 0 K

Boundary	θ	γ(mJ/m^2)	Boundary	θ	γ(mJ/m^2)
∑101(10 1 0)	11.4°	688	∑73(11 5 0)	48.9°	992
∑65(8 1 0)	14.3°	747	∑5(2 1 0)	53.1°	955
∑25(7 1 0)	16.3°	802	∑17(5 3 0)	61.9°	860
∑37(6 1 0)	18.9°	842	∑13(3 2 0)	67.4°	796
∑13(5 1 0)	22.6°	883	∑37(7 5 0)	71.1°	742
∑17(4 1 0)	28.1°	923	∑25(4 3 0)	73.7°	683
∑5(3 1 0)	36.9°	925	∑41(5 4 0)	77.3°	610
∑73(8 3 0)	41.1°	970	∑61(6 5 0)	79.6°	549

In this study, the MD simulation was carried out using the LAMMPS software with the embedded-atom method (EAM) potentials for Cu developed by Mishin et al. [53], which can fit a large set of experimental and first-principles data. The simulation temperature was controlled by the isothermal-isobaric (NPT) ensemble, Nose-Hoover thermostat, with zero pressure in each direction. The MD integration time step was set to 1 fs throughout the simulation.

In MD simulations of GBs, the configuration having the global minimum energy is always regarded as the merited boundary structure. However there is no assurance that the global minimum energy structure is the only configuration existing in the real materials [54, 55]. In the present study, different GB structures have been obtained by changing the initial distance between the upper and lower grains at the boundary plane, as illustrated in Figure 2. The upper grain moved up or down from the centre, shown in Figure 2(b). Seven distances of separation (3 Å, 2 Å, 1 Å, 0 Å, -1 Å, -2 Å and -3 Å) have been tested. A negative separation means that there is an overlap between the two grains. The overlap between the grains may result in an unphysically short distance between two atoms. If the distance between two atoms of different grains was less than the cutoff, then one atom was arbitrarily deleted in the upper grain. Following the movement of the upper grain, the bicrystal system was subject to energy minimization by molecular statics approach with a standard conjugate-gradient algorithm to reach the equilibrated GB structure. The GB energy was calculated after each energy minimization process. The optimized structures obtained were then subjected to a MD annealing procedure at desired temperature and zero stress state for 10ps to ensure their stability.

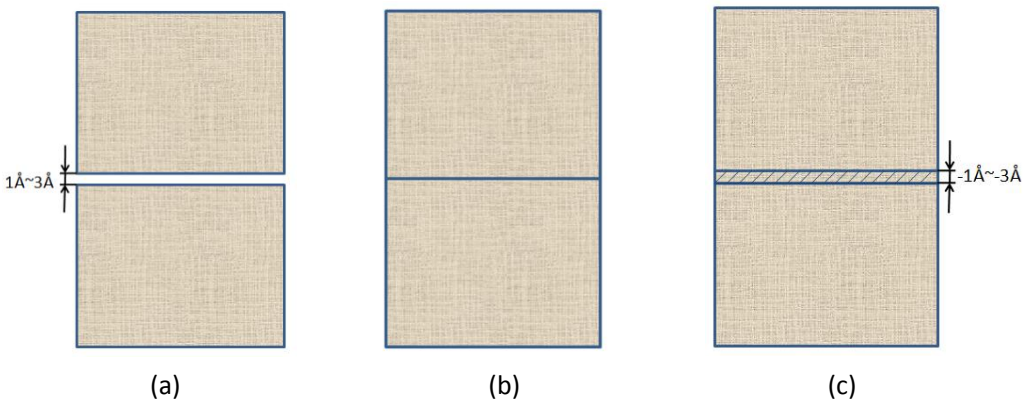

Figure 2 Schematic of the initial distance between the upper and lower grain at the boundary plane. (a) 1Å to 3 Å separation (b) perfect joining (c) 1Å to 3 Å overlap.

The visualization tool Atomeye [56] and Ovito [57] were used to produce illustration of the bicrystal models. The common neighbor analysis (CNA) technique [58] was used to identify the defect structure and its evolution during the simulations. Three categories of atoms with perfect face centered cubic (FCC) structure, hexagonal close packed (HCP) structure and other structures could be identified.

Once the equilibrium state of GB was reached, a shear deformation was applied to bicrystal model at 10 K to

investigate the GB migration and its coupled motion, as schemed in Figure 3. Atoms on the top of upper grain and atoms at the bottom of lower grain are fixed, the thickness of each fixed slab is about twice the cutoff radius of atomic interactions [53], all the other atoms in the model are set free. A constant shear velocity ν_s=1m/s parallel to the boundary plane was applied along the X direction on the atoms in the fixed area of upper grain while the fixed atoms in the lower grain keep stationary. The stress and temperature calculations were performed on the dynamic atoms between the fixed two slabs, stress tensor was calculated by the standard virial expression. In this study, the tangential translation of the grain can induce normal motion of the GBs. The position of GB was followed by calculating the average position of the disordered atoms along the boundary plane.

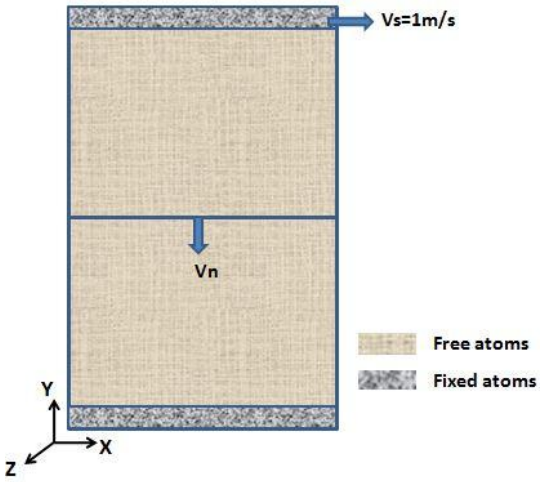

Figure 3 Schematic of the bicrystal model in dynamic simulation under shear force. ν_s and ν_n are the velocities of grain tangential translation and GB normal motion respectively.

3. Results and discussion

3.1 GB structure and energy

Figure 4(a) and Figure 4(b) respectively show the specific GB energies (GB energies per unit GB area) as a function of the moving distance of the upper grain for a low-angle ∑101 (10 1 0) (θ=11.4°) GB and a high-angle ∑5 (3 1 0) (θ=36.9°) GB. The corresponding GB structures are also displayed in the figures. For the ∑101 (10 1 0) GB, the specific GB energy varies from 688 mJ/m^2 to 744 mJ/m^2. The low tilt angle fostered a wider range of GB structures. Five different grain boundary structures have been observed for this low-angle GB, as shown in Figure 4(a). The normal-kite units (S1), the long-kite units (S3) and other three rotated-kite units (S2, S4 and S5) were identified. For the ∑5 (3 1 0) GB, the specific GB energy varies from 925 mJ/m^2 to 1217 mJ/m^2 and only two different types of grain boundary structures have been observed, namely the normal-kite units (S1) and the split-kite units (S2), as shown in Figure 4(b). Different initial separation/overlapping of two grains could result in the same GB structure and same GB energy. The GB structure with the lowest energy is regarded as the equilibrium structure, while other GB structures with higher GB energy are reckoned to be metastable. It can be seen from Figure 4 that the normal-kite structure is the equilibrium structure for both the low-angle GB and the high-angle GB.

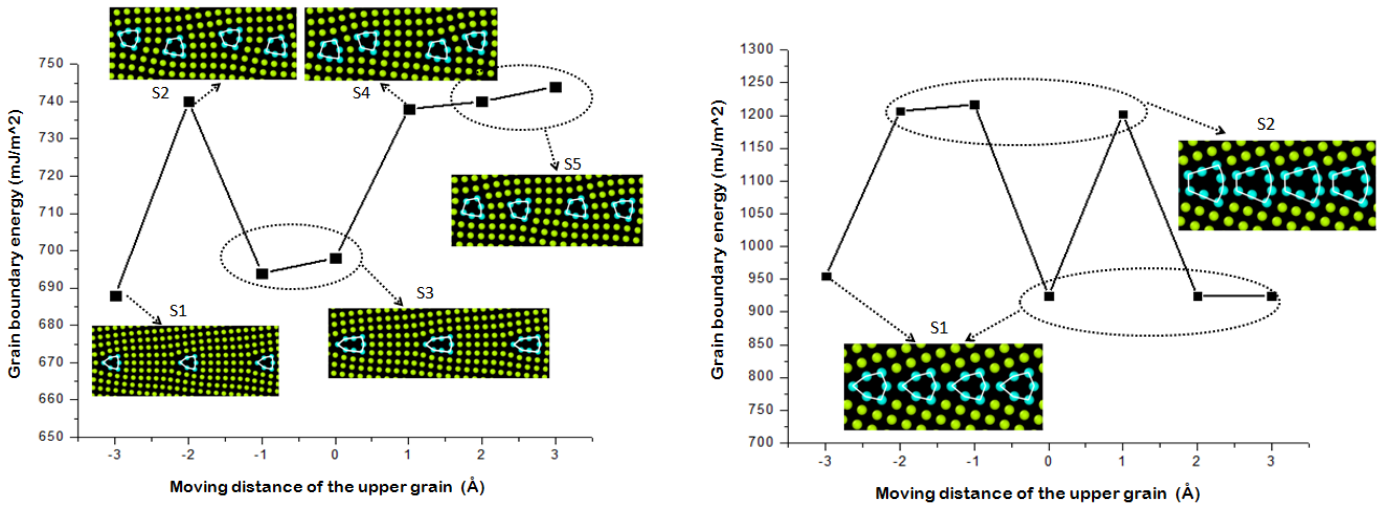

Figure 4 Energy and the corresponding structures of (a) ∑101 (10 1 0) (θ=11.4°) GB and (b) ∑5 (3 1 0) (θ=36.9°) GB after energy minimization at 0K based on different moving distances of the upper grain.

The specific GB energies for the 0K equilibrium structures is presented as a function of tilt angle (θ) in Figure 5. The specific GB energies calculated in this work are compared with the results predicted by Mishin et al. [10]. It can be seen that the two sets of results match each other very well. The difference slightly increases at both ends of the curves.

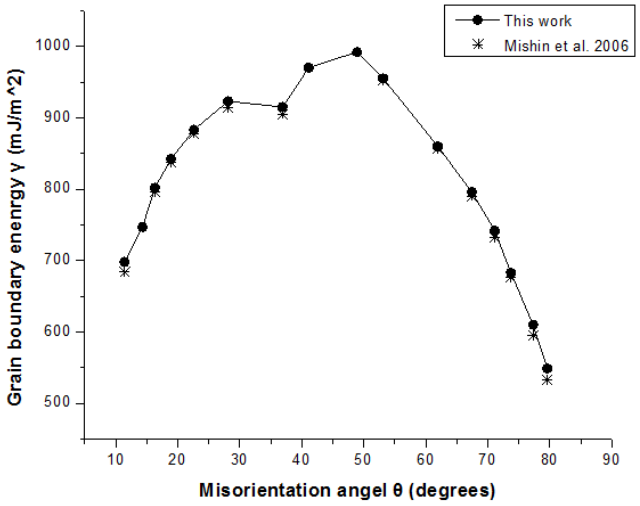

Figure 5 Grain boundary energy γ as a function of the misorientation angle θ of the equilibrium GB structures. The sixteen values calculated in this work are compared with the thirteen calculated value by Mishin's [10].

Eight simulated GB structures are shown in Figure 6(a)-(h). The corresponding tilt angle varies from 11.4° to 79.6°. The black and white balls correspond to the two adjacent atom layers along the tilt axis. All the [0 0 1] tilt GBs contain topologically identical kite-shaped structural units. They differ only by the distance separating the kites and by their positions relative to the GB plane. As defined in [59], the kite-shaped units containing six atoms are referred to "E" unit marked in the figures. The E units approach each other with an increasing misorientation angle when θ＜53.1°. The distance between adjacent units increases when θ＞53.1°, forming either a flat (Figure 6(h)) or a zigzag (Figure 6(f),(g)) boundary plane. The relatively low-angle GBs, such as the ∑101 (10 1 0) (θ=11.4°) and ∑61 (6 5 0) (θ=79.6°), contains an array of dislocations whose cores are formed by the E unit. the Burgers vectors are b=[1 0 0] and b=-1/2[1 1 0] for these two cases respectively. The Burgers vectors of the dislocations are determined by the standard Burgers circuit, as marked in Figure 6(a) and Figure 6(h). Among the investigated sixteen GBs, two special GB structures are found as outlined in Figure 6(b) and Figure 6(d). The equilibrium GB structure of ∑25 (7 1 0) (θ=16.3°) is composed of an array of long-kite shaped structural units E_1 with 8 atoms included in each unit. The ∑73 (8 3 0) (θ=41.1°) boundary presents another special case: a short-kite E_2 unit was present every two E units. These special boundary structures will result in a

different mechanism of boundary motion, which will be specified after.

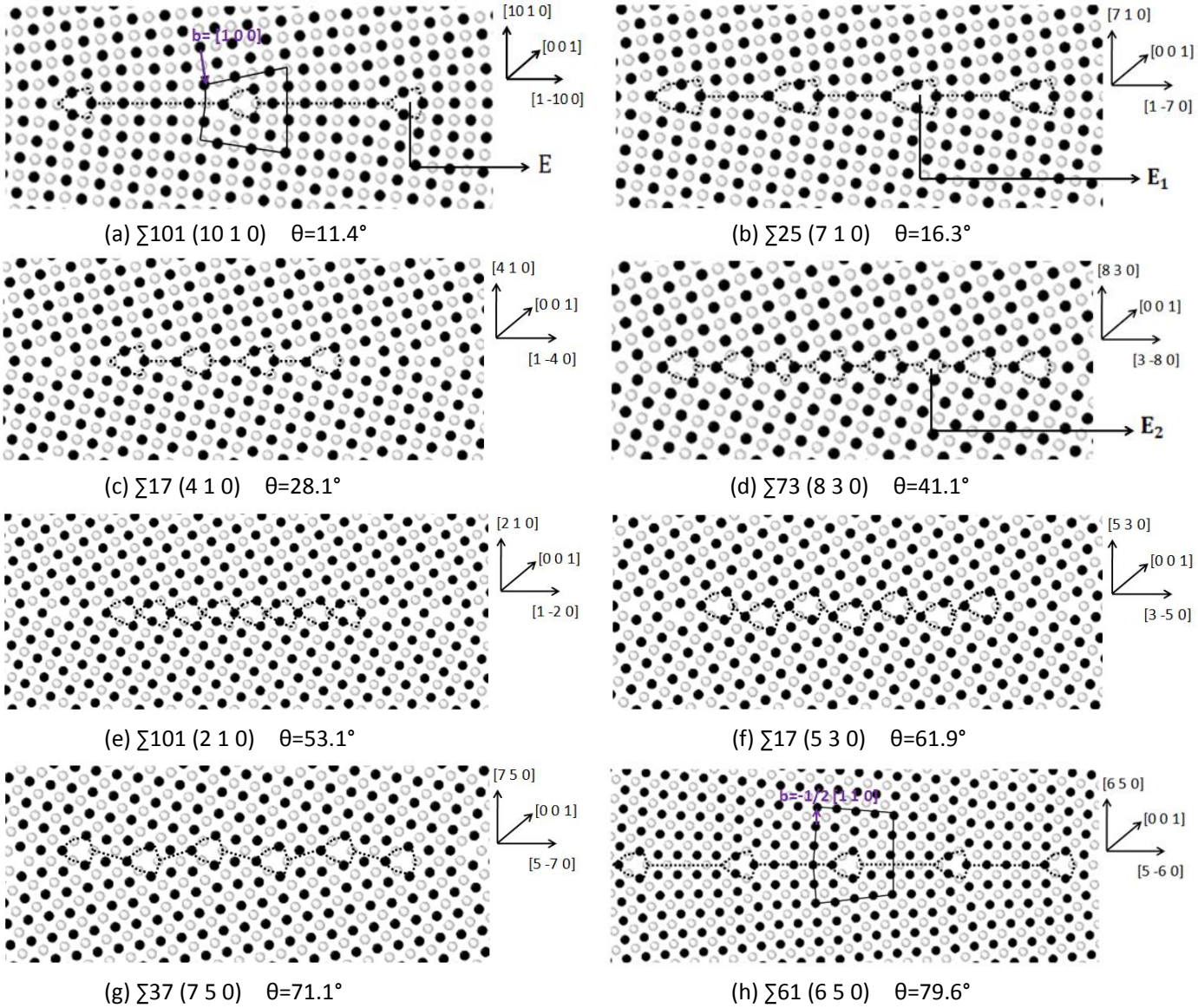

Figure 6 Eight GB structures in Cu for various misorientation angles θ at 0K. The structures are viewed along the [0 0 1] tilt axis. Atoms on consecutive (0 0 2) planes are shown as black and white. The GB normal for the upper and lower grain are marked on the right-hand side for each GB. The structure units at each boundary plane are outlined by the dash line.

3.2 GB coupling motion

Some [0 0 1] symmetrical tilt GBs can couple to applied shear stress and be moved by them has been well confirmed in previous experimental[45, 60] and simulation studies[10, 61]. In this work, MD simulation results demonstrate that all the investigated [0 0 1] tilt GBs can show a migrating motion coupled to the shear strain when the stress reached a critical level. Figure 7 shows the stress and GB position versus the simulation time of four selected cases. At a coarse scale, the GB displacement is a linear function of the simulation time for these four GBs cases. This linear relation can be used to estimate the coupling factor β, the ratio of the tangential grain translation to the associated normal GB displacement, or the tangential and normal velocity.

It is clear from Figure 7 that the GB motion is intermittent during the migration. The boundary jumps abruptly to the equilibrium position. It remains in this configuration until the local energy barrier is consecutively overcome to reach the next local energy minimum. The boundary plane is not perfectly stationary between jumps but vibrates at a very slow rate near the equilibrium position because of the anisotropic elastic strain in each of the two grains. Simulation results have also reveals the dynamics of stress-driven GB motion. The GB motion exhibits stick-slip behavior characterized by a saw-tooth time dependence of the stress and a stop-and -go character of the motion, as seen in Figure 7. Specifically, when the GB is stationary, the system's stress builds up at a fixed rate until the accumulated stress is large enough to drive

the boundary to move. The grain boundary jumped abruptly at the peak stress while the build-up stress was relieved to a lower level. This periodic process kept driving the motion of the boundary and resulted in the growth of one grain and the shrinkage of the other one. For each stress cycle, the boundary was stationary for 50 to 100 ps while one migration step was completed in a few ps.

The stress increased at a fixed rate any time the boundary was still, implying that there was no sliding between the two grains during the migration process. Furthermore, the abrupt jump of the boundary plane represents the collective motion of the boundary atoms and suggests that the coupled grain boundary motion does not involve diffusion under athermal condition, which can implement by lattice deformation and rotation. The macroscopic mechanisms for the coupled motion of [0 0 1] symmetric tilt GBs is quite straightforward: the shear strain increases the stress in the grain and induces the boundary to migrate. In turn, the GB migration releases the stress stored in the deformed grain.

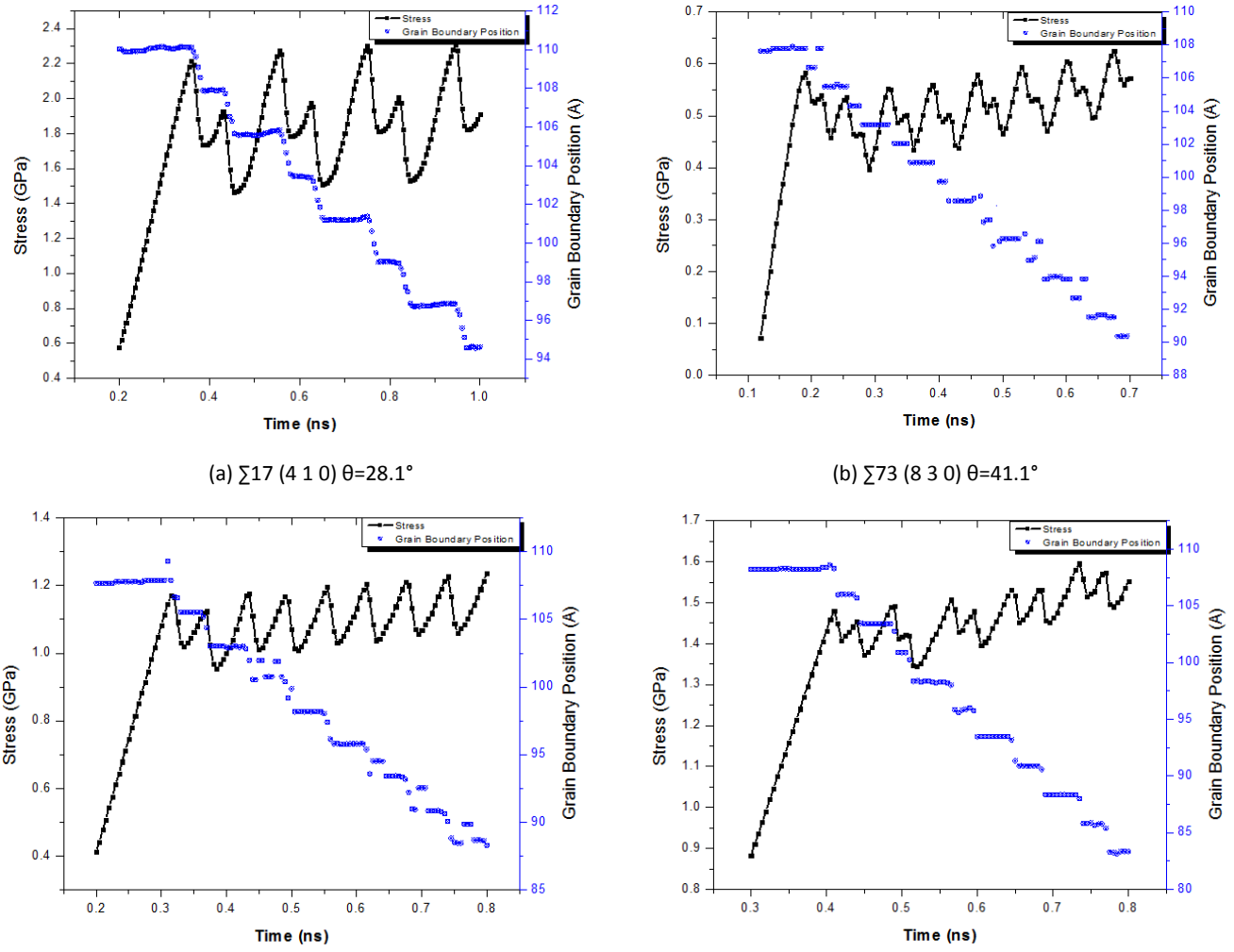

(a) ∑17 (4 1 0) θ=28.1°

(b) ∑73 (8 3 0) θ=41.1°

(c) ∑5 (2 1 0) θ=53.1°

(d) ∑13 (3 2 0) θ=67.4°

Figure 7 Shear stress and grain boundary position versus simulation time of four bicrystal system at 10K. The grain boundary positions are followed by calculating the average position of the disordered atoms at the boundary plane.

3.3 Atomic mechanisms of GB migration

The mechanism of GB migration at atomic-scale and their dependence to the boundary structures are now examined. The atomic mechanisms were considered by observing continuous snapshots of the MD simulation along with the moving trajectories of each atom in the structure unit.

A typical mechanism is illustrated in Figure 8 for the ∑5 (3 1 0) GB. The E and E' units are outlined by the dashed line. The two units are topologically the same since they can be transformed by relatively small in-plane atomic displacements. Both of them contain 6 atoms which are referenced in Figure 8(a) by the indexes 1 to 6 in the E unit and $1'$ to $6'$ in the E' unit. The two structural units share two atoms, namely the atoms 5 and 6 in the E unit and the atoms $2'$ and $1'$ in the E' unit. It can be seen in Figure 8(a) that the atoms 2 and 3 align in a vertical line in the original E unit,

while the atoms 4 and 6 align along another vertical line. As the shear deformation proceeds, the atoms move out of their E vertical lines, as shown in Figure 8(c). Meanwhile, the distance between the atoms $2'$ and $3'$ in the E' unit increases in the vertical direction, but decreases in the horizontal direction. The atoms $4'$ and $6'$ have similar movement. Once the atoms $2'$ and $3'$ as well as the atoms $4'$ and $6'$ align along the vertical direction, the E—E' transformation is complete . Thus, the grain boundary completed a down-step movement.

Another typical mechanism of the coupling motion is shown in Figure 9 using the zigzag ∑37 (7 5 0) GB as an example. Similar to the ∑5 (3 1 0) GB, the E and E' units in ∑37 (7 5 0) GB share two atoms as well. However, the shared atoms in this GB are different to the ∑5 (3 1 0) GB. They are the atoms 3 and 6 in the E unit and the atoms $2'$ and $4'$ in the E' unit. The relative location of the E unit and E' unit is also different in the ∑37 (7 5 0) GB and ∑5 (3 1 0) GB. The E' unit is located right below or above the E unit in the ∑37 (7 5 0) GB. However E' is located on the side of the E unit in the ∑5 (3 1 0) GB. The difference in the relative location of the two units results in different atomic coupling mechanisms. The ∑5 (3 1 0) GB has a flat GB plane, in which the boundary displacements take place collectively over the entire GB area. However, the process of E—E' transition in the zigzag ∑37 (7 5 0) GB boundary is alternative. Specifically, atom $4'$ in E' unit firstly moves to the horizontal line with atom $2'$, the transition in this process results in a mirrored symmetric structure of E and E' units, as shown in Figure 9(b). As the shear deformation proceeds, the distance between the atoms $2'$ and $3'$ as well as atoms $4'$ and $6'$ in the E' unit increases in the vertical direction, but decreases in the horizontal direction. Once the atoms $2'$ and $3'$, atoms $4'$ and $6'$ align in a vertical line in the E' unit, the E—E' transformation is complete, the higher E unit in the middle in Figure 9(a) moves one step down while the other two E units are still at the original positions as shown in Figure 9(c). The stationary E units stand at a higher level along the Y direction than the displaced E units after one transition and they will move down in the next migration cycle.

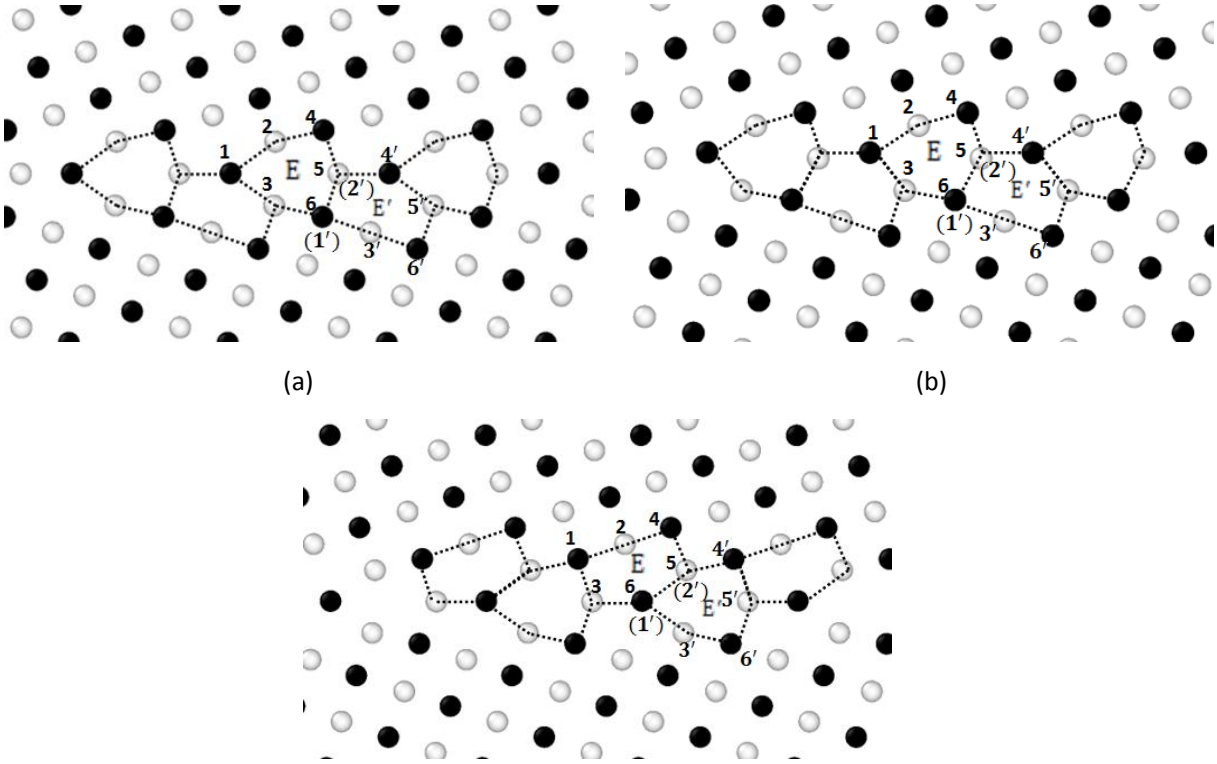

Figure 8 Atomic mechanism of coupled motion of the ∑5 (3 1 0) GB. (a),(b), (c) are the initial, transition and final state during one step of GB migration.

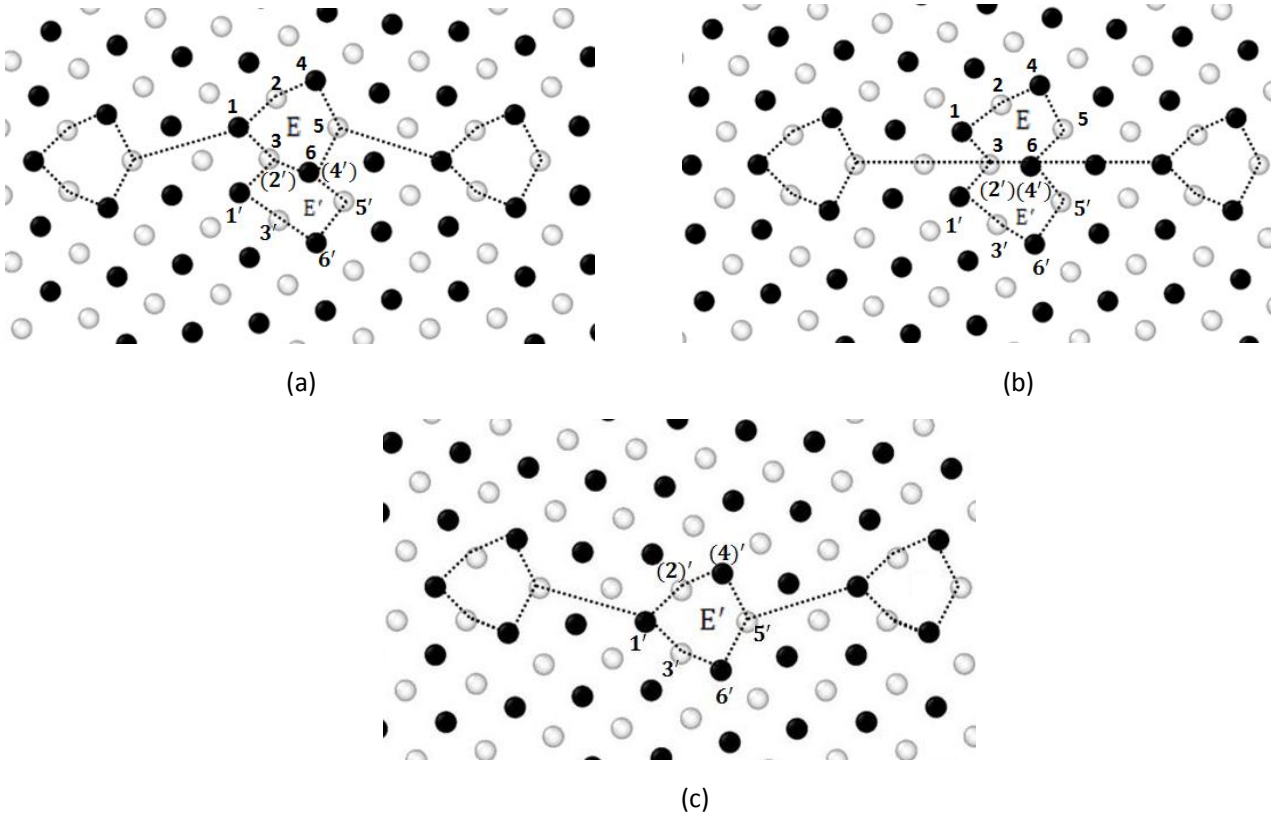

Figure 9 Atomic mechanism of coupled motion of the ∑37 (7 5 0) GB. (a), (b), (c) are the initial, transition and final state during one step of GB migration.

This normal kite unit dominates the equilibrium structure of most [0 0 1] symmetric tilt GBs except for ∑17(4 1 0) and ∑73 (8 3 0) GBs. In the latters the structural phase transformation of GB are observed during the coupling motion. This results in different atomic coupling mechanisms as schemed in Figure 10 and Figure 11.

For ∑17(4 1 0) GB, the initial equilibrium boundary plane in Figure 10(a) is organized by an array of normal-kite E structural units. As the shear deformation proceeds, atoms 2 and 4 move out of their vertical lines with atoms 3 and 6 in the E unit while atom 5 in E unit and atoms $2'$ and $4'$ in E' move to the right gradually. When these move in the vertical line with the atoms $1'$, $3'$ and $6'$, the long-kite unit E_1 is formed and replaces the normal-kite E to construct the new boundary plane, as outlined by the solid line in Figure 10(b). The newly formed E_1 unit (organized by atom 6, 5, 1, $2'$, $3'$, $4'$, $5'$, and $6'$) can be regarded as the combination of the deformed E unit and E' unit, recall that this long-kite unit was found in the equilibrium structure of ∑25 (7 1 0) GB in Figure 6(b) and the metastable structure of ∑101 (10 1 0) GB in Figure 4(a). The structural phase transformation of GB results in a down-step movement of GB. This new boundary structure is not stable. It is easily transformed into the initial GB configuration as the shear deformation increases. This process is realized by the transition of the E' unit in Figure 10(b) to the E unit in Figure 10(c). Alternatively it can be regarded as the decomposition of the E_1 into two E units, since the atoms marked 3, 6 and $1'$ in one E unit and atoms marked $6'$ and $5'$ in another E unit in Figure 10(c) are from the same E_1 unit in Figure 10(b). This structural transformation back to the initial GB configuration leads to another down-step movement of GB.

Figure 11 shows another style of boundary transformation in ∑25 (7 1 0) GB during the migration. The initial equilibrium GB plane is made of normal-kite E units and short-kite E_2 units. The periodic boundary structure is "⋯ E- E-E_2- E- E-E_2⋯". The E' units can be found between any two E units or between the E unit and E_2 unit, as seen in Figure 11(a). With the increased shear strain, all the E' units transform to E units to form a new boundary plane. The new GB plane is made of E units only and the periodic structure now is "⋯E- E E- E- E E- E⋯". In order to contrast with the initial configuration, the transformed normal-kite E unit is still marked with E', as outlined in Figure 11(b). As for the case involving ∑17(4 1 0) GB, the new GB plane is just a structure of transition. The new plane soon turns back to the initial structure with further increased of the shear strain as seen in Figure 11(c). Each GB structural phase transformation will result in GB to move one step down. For both the ∑17(4 1 0) GB case and the ∑25 (7 1 0) GB case, the boundary transformation is carried out alternately during the process of GB coupling motion.

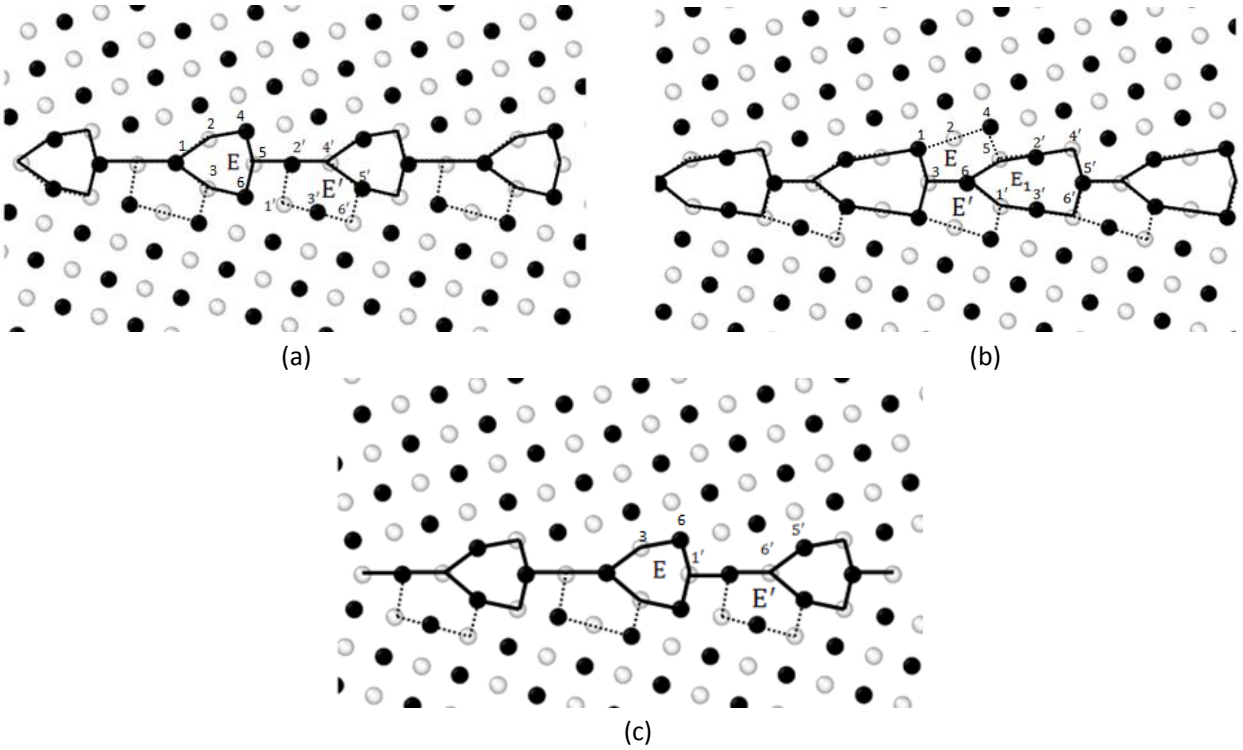

Figure 10 Atomic mechanism of coupled motion of ∑17 (4 1 0) GB. Two different GB structures are outlined by the solid line.

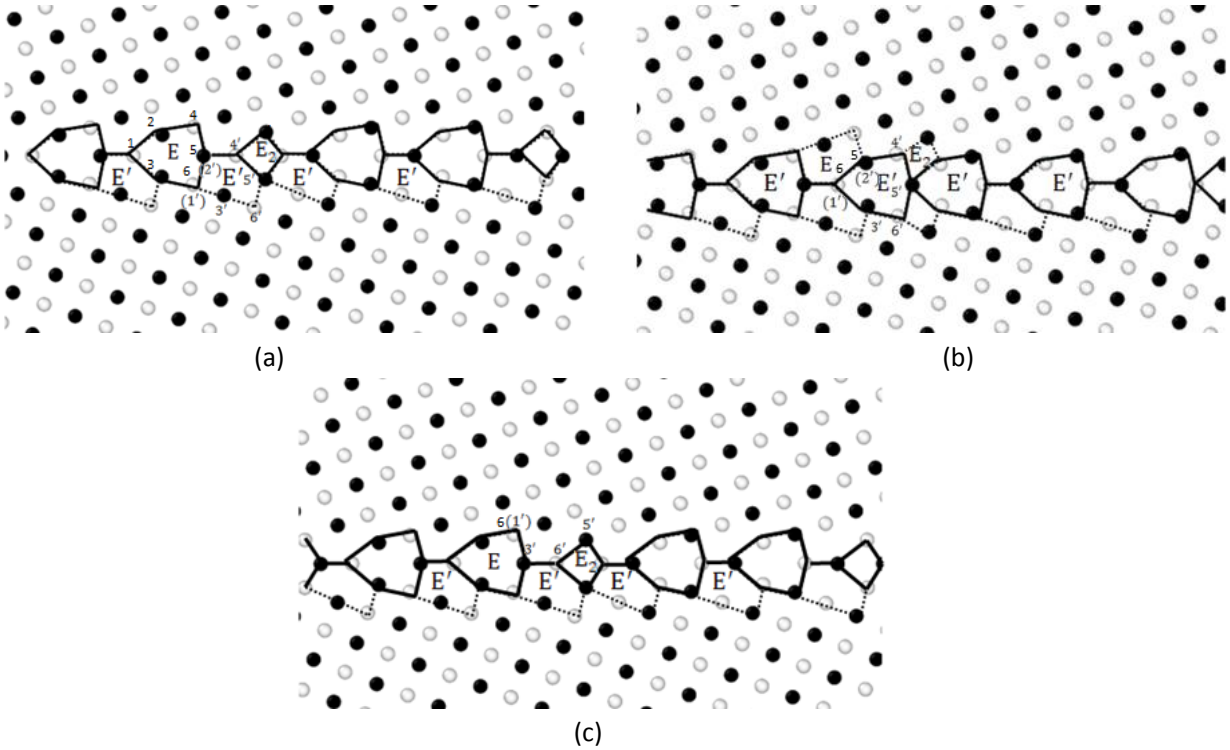

Figure 11 Atomic mechanism of coupled motion of ∑73 (8 3 0) GB. Two different GB structures are outlined by the solid line.

The descriptions above give us a deep insight into the mechanisms of grain boundary migration coupled to the mechanisms of shear deformation at atomic scale. In summary, the migration is achieved by conversion of atomic lattice units of one crystal into structural units of the other crystal which are differently oriented and located. The common idea of these mechanisms can be regarded as the displacement of local atoms and rotation of the atomic groups in GB structural units.

6. Conclusion

Molecular statics and molecular dynamics simulations using the EAM interatomic potential are carried out to study the structures and the coupling motion of sixteen [0 0 1] symmetric tilt grain boundaries in Cu bicrystal.

A general method is proposed to explore the possible GB structures. Molecular statics simulation at 0K proved that,

by changing the initial distance between the upper and lower grain, different GB structures can be obtained based on a certain misorientation angle θ of the bicrystal model. With this method, the equilibrium and some of the possible metastable structures of the investigated [0 0 1] GBs are determined. Compared with high-angle boundaries, the structure of low-angle boundaries are unstable. The instabilities gave rise to a wider variety of boundary configurations in the simulations. All the equilibrium structures presented in this work were based on an energetic point of view. They are the most thermodynamically favorable GB structures. The stability of the equilibrium structures found at 0K does not guarantee that structures with higher energies do not exist in the real materials.

Molecular Dynamics simulations were conducted on the equilibrium bicrystal systems by applying a shear strain parallel to the grain boundary plane. The computational results show that all the GBs can migrate coupled to the shear deformation and the boundary migration is embedded within a stick-slip mechanism. The analysis of the atomic mechanisms of GB coupling motion highlighted that the $\mathrm{E}-\mathrm{E}'$ structure transformation prevailed in all of the [0 0 1] GBs. The transformation of the structural phase was found during the migration of ∑17(4 1 0) and ∑73 (8 3 0) GBs. The common feature of the mechanisms is the displacement and rotation of certain structural units in both grains that leads to the assimilation of the atomic lattice units of one grain into the structural units of the other grain.

Acknowledgements

This work was supported by an Australia Research Council Discovery Grant (DP0773329). Simulations were performed using the HPC cluster of University of Wollongong and the computing facilities provided by NCI National Facility of Australia. Liang Zhang would like to acknowledge the financial support from China Scholarship Council (CSC).

References

[1] A.P. Sutton, R.W. Balluffi, Interfaces in crystalline materials, Clarendon, Oxford, 1995.
[2] R.J. Asaro, P. Krysl, B. Kad, Philosophical Magazine Letters, 83 (2003) 733-743.
[3] C.C. Koch, Scripta Materialia, 49 (2003) 657-662.
[4] K.S. Kumar, H. Van Swygenhoven, S. Suresh, Acta Materialia, 51 (2003) 5743-5774.
[5] H. Van Swygenhoven, Science, 296 (2002) 66-67.
[6] H. Van Swygenhoven, P.M. Derlet, Physical Review B, 64 (2001).
[7] E. Ma, Science, 305 (2004) 623-624.
[8] Z. Shan, E.A. Stach, J.M.K. Wiezorek, J.A. Knapp, D.M. Follstaedt, S.X. Mao, Science, 305 (2004) 654-657.
[9] V. Yamakov, D. Wolf, S.R. Phillpot, H. Gleiter, Acta Materialia, 50 (2002) 61-73.
[10] J.W. Cahn, Y. Mishin, A. Suzuki, Acta Materialia, 54 (2006) 4953-4975.
[11] T. Gorkaya, D.A. Molodov, G. Gottstein, Acta Materialia, 57 (2009) 5396-5405.
[12] D.A. Molodov, T. Gorkaya, G. Gottstein, Scripta Materialia, 65 (2011) 990-993.
[13] Z. Budrovic, H. Van Swygenhoven, P.M. Derlet, S. Van Petegem, B. Schmitt, Science, 304 (2004) 273-276.
[14] K.S. Kumar, S. Suresh, M.F. Chisholm, J.A. Horton, P. Wang, Acta Materialia, 51 (2003) 387-405.
[15] X.Z. Liao, F. Zhou, E.J. Lavernia, S.G. Srinivasan, M.I. Baskes, D.W. He, Y.T. Zhu, Applied Physics Letters, 83 (2003) 632-634.
[16] H. Van Swygenhoven, P.M. Derlet, A.G. Frøseth, Acta Materialia, 54 (2006) 1975-1983.
[17] H. Van Swygenhoven, P.M. Derlet, A. Hasnaoui, Physical Review B, 66 (2002).
[18] T. Mori, H. Miura, T. Tokita, J. Haji, M. Kato, Philosophical Magazine Letters, 58 (1988) 11-15.
[19] T. Mori, T. Ishii, M. Kajihara, M. Kato, Philosophical Magazine Letters, 75 (1997) 367-370.
[20] V. Randle, Acta Materialia, 46 (1998) 1459-1480.
[21] V. Randle, P. Davies, Interface Science, 7 (1999) 5-13.
[22] G. Duscher, M.F. Chisholm, U. Alber, M. Rühle, Nature Materials, 3 (2004) 621-626.
[23] F. Lancon, T. Radetic, U. Dahmen, Physical Review B, 69 (2004).
[24] H. Nishimura, K. Matsunaga, T. Saito, T. Yamamoto, Y. Ikuhara, Journal of the American Ceramic Society, 86 (2003) 574-580.
[25] D. Wolf, Acta Metallurgica, 37 (1989) 1983-1993.
[26] D. Wolf, Acta Metallurgica, 37 (1989) 2823-2833.
[27] D. Wolf, Acta Metallurgica, 38 (1990) 781-790.
[28] D. Wolf, Acta Metallurgica, 38 (1990) 791-798.

[29] J.D. Rittner, D.N. Seidman, Physical Review B, 54 (1996).
[30] M.D. Sangid, H. Sehitoglu, H.J. Maier, T. Niendorf, Materials Science & Engineering A, 527 (2010) 7115-7125.
[31] C.H. Li, E.H. Edwards, J. Washburn, E.R. Parker, Acta Metallurgica, 1 (1953) 223-229.
[32] D.W. Bainbridge, H.L. Choh, E. H. Edwards, Acta Metallurgica, 2 (1954) 322-333.
[33] D.A. Molodov, T. Gorkaya, G. Gottstein, Journal of Materials Science, 46 (2011) 4318-4326.
[34] T. Gorkaya, K.D. Molodov, D.A. Molodov, G. Gottstein, Acta Materialia, 59 (2011) 5674-5680.
[35] M. Winning, G. Gottstein, L.S. Shvindlerman, Acta Materialia, 49 (2001) 211-219.
[36] H. Yoshida, K. Yokoyama, N. Shibata, Y. Ikuhara, T. Sakuma, Acta Materialia, 52 (2004) 2349-2357.
[37] F. Mompiou, D. Caillard, M. Legros, Acta Materialia, 57 (2009) 2198-2209.
[38] T. Gorkaya, T. Burlet, D.A. Molodov, G. Gottstein, Scripta Materialia, 63 (2010) 633-636.
[39] F. Mompiou, M. Legros, D. Caillard, Journal of Materials Science, 46 (2011) 4308-4313.
[40] M. Legros, D.S. Gianola, K.J. Hemker, Acta Materialia, 56 (2008) 3380-3393.
[41] D.S. Gianola, C. Eben, X. Cheng, K.J. Hemker, Advanced Materials, 20 (2008) 303-308.
[42] J.W. Cahn, Y. Mishin, International Journal of Materials Research, 100 (2009) 510-515.
[43] Y. Mishin, A. Suzuki, B.P. Uberuaga, A.F. Voter, Physical Review B, 75 (2007).
[44] J.W. Cahn, Y. Mishin, A. Suzuki, Philosophical Magazine, 86 (2006) 3965-3980.
[45] D.A. Molodov, V.A. Ivanov, G. Gottstein, Acta Materialia, 55 (2007) 1843-1848.
[46] M. Winning, Philosophical Magazine, 87 (2007) 5017-5031.
[47] D.E. Spearot, K.I. Jacob, D.L. McDowell, Acta Materialia, 53 (2005) 3579-3589.
[48] D.E. Spearot, K.I. Jacob, D.L. McDowell, S.J. Plimpton, Journal of Engineering Materials and Technology-Transactions of the ASME, 127 (2005) 374-382.
[49] F. Sansoz, J.F. Molinari, Scripta Materialia, 50 (2004) 1283-1288.
[50] F. Sansoz, J.F. Molinari, Acta Materialia, 53 (2005) 1931-1944.
[51] D.E. Spearot, K.I. Jacob, D.L. McDowell, International Journal of Plasticity, 23 (2007) 143-160.
[52] V. Yamakov, D. Wolf, M. Salazar, S.R. Phillpot, H. Gleiter, Acta Materialia, 49 (2001) 2713-2722.
[53] Y. Mishin, M.J. Mehl, D.A. Papaconstantopoulos, A.F. Voter, J.D. Kress, Physical Review B, 63 (2001).
[54] G.H. Campbell, S.M. Foiles, P. Gumbsch, M. Rühle, W.E. King, Physical Review Letters, 70 (1993) 449-452.
[55] M. Elkajbaji, J. Thibault, H.O.K. Kirchner, Philosophical Magazine Letters, 73 (1996) 5-10.
[56] J. Li, Modelling and Simulation in Materials Science and Engineering, 11 (2003) 173-177.
[57] A. Stukowski, Modelling and Simulation in Materials Science and Engineering, 18 (2010) 015012-015017.
[58] J. Schiøtz, F.D. Di Tolla, K.W. Jacobsen, Nature, 391 (1998) 561-563.
[59] J.D.S.D.N. Rittner, Physical Review, B, 54 (1996).
[60] T. Gorkaya, D.A. Molodov, G. Gottstein, Acta Materialia, 57 (2009) 5396-5405.
[61] M. Shiga, W. Shinoda, Physical Review B, 70 (2004).